ARCHIVES of FOUNDRY ENGINEERING

Published quarterly as the organ of the Foundry Commission of the Polish Academy of Sciences

ISSN (1897-3310)
Volume 14
Issue 3/2014

87 – 92

18/3

A Study of Effects of Precipitation Hardening of Low-Alloy Copper-Nickel Spheroidal Cast Iron

T. Szykowny *, T. Giętka, Ł. Romanowski, M. Trepczyńska-Łent
Department of Materials Science and Engineering, University of Technology and Life Sciences
Prof. S. Kaliski 7, 85-796 Bydgoszcz, Poland
*Corresponding author. E-mail address: tadeusz.szykowny@utp.edu.pl

Received 28.04.2014; accepted in revised form 15.05.2014

Abstract

One type of spheroidal cast iron, with additions of 0.51% Cu and 0.72% Ni, was subjected to precipitation hardening. Assuming that the greatest increase in hardness after the shortest time of ageing is facilitated by chemical homogenisation and fragmentation of cast iron grain matrix, precipitation hardening after pre-normalisation was executed. Hardness (HB), microhardness (HV), qualitative and quantitative metalographic (LM, SEM) and X-ray structural (XRD) tests were performed. The acquired result of 13.2% increase in hardness after ca. 5-hour ageing of pre-normalised cast iron confirmed the assumption.

Keywords: Heat treatment, Low-alloy spheroidal cast iron, Precipitation hardening

1. Introduction

Precipitation hardening of iron and copper alloys is possible thanks to the copper solubility in α iron increasing with the rise of temperature. The maximum copper solubility in iron reaches 2.2% m/m at 850^{o}C, the eutectoid transformation temperature [1]. Exceeding the threshold saturation results in precipitating the copper excess in the form of ε phase. It is a solid threshold solution of iron in copper, with a 98.9% m/m content of Cu. The ε phase crystallises in an A1 lattice. The copper dissolved in iron causes the solvent structure to expand, in accordance with Vegard's law [2-3]. The dispersion precipitates of the ε phase are a factor that strengthens the alloy. The precipitate dimensions do not depend under the given ageing conditions (temperature, time) from the copper content in the alloy [4]. Precipitation hardening is a routine thermal treatment of low-carbon, low-alloy HSLA (High Strength Low Alloy) steel. The very low content of carbon provides good weldability of this type of steel, and the required level of resilience properties is achieved by precipitation hardening. Aside from copper, HSLA steel also contains alloy additions such as Ni, Cr, Mo, Mn, but copper plays the primary role in precipitation hardening [5-10].

As an alloy addition in cast iron, copper is used in order to increase the pearlite content, which noticeably improves the resilience properties, at the same time reducing plasticity and impact strength [11]. Copper content in cast iron usually does not exceed 2% m/m. At copper content of ca. 2%, spheroidal cast iron is completely pearlitic [12]. An addition of nickel, similarly to copper, facilitates the eutectoid transformation of austenite into pearlite. Nickel and copper (at lower contents) do not stabilise eutectoid cementite, i.e. do not prevent intermediate graphitisation [13].

The presence of copper in cast iron's chemical composition can be used for precipitation hardening [14-18]. In the case of cast iron with a lower copper content and no cementite-stabilising

additions, matrix ferritisation occurs during oversaturation. The lowering of resilience properties as a result of ferritisation is mostly compensated by the following effect of ageing.

In paper [18], cast iron with a 0.48% Cu content and ferritic matrix, after 32 hours of ageing under 450°C, acquired an Rm strength greater than 500 MPa, with unit elongation of ca. 23%. The long time of ageing that led to acquiring the significant increase in resilience and hardness seems to be the primary obstacle in the way of greater popularisation of the presented treatment. Pre-normalisation of cast iron with increased copper content (2.1% Cu) resulted in a 26% increase in hardness even after 4 hours of ageing [19].

The goal of the paper is to determine the influence of preliminary thermal treatments on the kinetics and maximum effects of ageing of precipitation hardened low-alloy spheroidal cast iron.

2. Material, program and methodology of research

One type of low-alloy spheroidal cast iron was accepted for the research. The cast iron was smelted in a medium-frequency induction furnace with a 3.5 t capacity. Spheroidisation of the cast iron was performed using VL53M magnesium mortar (using bell method in a slender ladle), and modification - with FeSi75 ferrosilicon. The cast iron was cast into green-sand moulds replicating YII samples in accordance with PN-EN 1563:2012. 5-time resilience samples were made of cuboid ingots in accordance with PN-EN ISO 6892-1:2010. The result of the static stretch test is an average of three measurements. The HBW 2.5/187.5 hardness was measured at the heads of resilience samples. Cast iron chemical composition determined by spectroscopic means is presented in Table 1.

Table 1.
Cast iron chemical composition, % m/m

C	Si	Mn	P	S	Mg	Cu	Ni	Ti
3.39	2.62	0.29	0.042	0.010	0.046	0.51	0.72	0.011

The values of cast iron critical temperatures determined by dilatometry during constant heating and cooling at constant speed (0.019 K/s) are presented in Table 2. Mechanical properties and structural composition are presented in Table 3.

Table 2.
Values of moulded cast iron critical temperatures, °C

$Ac_{1,1}$	$Ac_{1,2}$	$Ar_{1,1}$	$Ar_{1,2}$	T_{gr}
788	862	820	729	732

Table 3.
Mechanical properties and cast iron structure

R_m, MPa	A_5, %	HB	Structure, % v/v			
			ferrite	pearlite	cementite	graphite
656	3.2	252	27.9	72.0	0.1	11.7

The structure of moulded cast iron is presented in Figure 1.

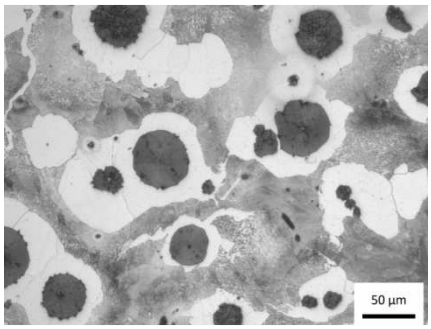

Fig. 1. Moulded cast iron microstructure, etched with 2% HNO_3

Moulded cast iron can be classified as grade EN-GJS-600-3 in accordance with the PN-EN 1563:2012 standard.

Three variants of precipitation hardening of cast iron have been assumed, designated S, N1 or N2, presented in a temperature-time system in Figures 2-4.

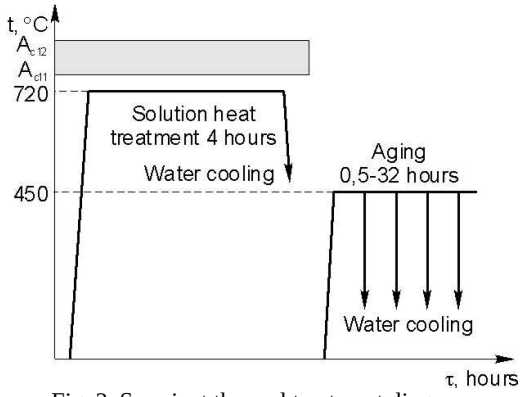

Fig. 2. S-variant thermal treatment diagram

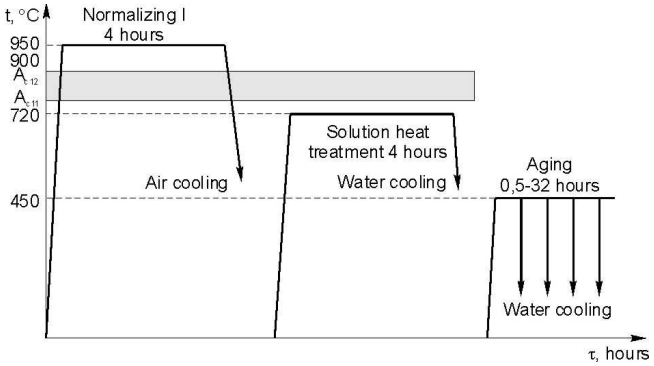

Fig. 3. N1-variant thermal treatment diagram

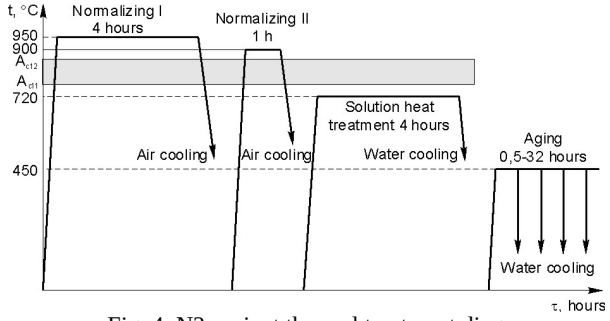

Fig. 4. N2-variant thermal treatment diagram

The operation of normalisation and oversaturation was performed on 10 mm tiles cut from YII sample casts. After oversaturation, the tiles were cut into 14x14x8 mm dice and aged for 0.5; 1; 2; 3; 4; 5; 6; 7; 8; 10; 12; 16; 24 or 32 hours. Normalisation and oversaturation was performed using a PSK-7 electric chamber furnace, while ageing in a bath furnace using SO 140 salt. Etched metallographic specimens were executed out of all samples. Quantitative microscopic analysis was performed on the recorded microstructure images using the NIS Elements 3.0 AR computer program. Images recorded using a Nikon Eclipse MA100 microscope were used. In order to determine ferrite grain size and pearlite inter-plate distance, metallographic tests on a JEOL JSM 5600 scanning microscope were performed. 5 hardness measurements were performed on each sample using Brinell 2.5/187.5 method and Struers Duramin 500 hardness meter. Ferrite and pearlite microhardness was determined using Vickers HV0.1 method and Hanemann lens. X-ray diffraction tests were performed on selected samples in order to measure the lattice parameter and the ferrite diffraction line half-width. Iron-filtered cobalt anode lamp radiation was used.

3. Test results with discussion

Normalised cast iron has pearlitic matrix with a small ferrite content in the form of incomplete, thin envelopes or non-continuous mesh (Fig. 5). Single-normalised cast iron from the 950°C temperature (N1) contains 0.7% ferrite Fig. 5a), while double-normalised (N2) from the 900°C temperature in the second normalisation treatment - 1.2% ferrite (Fig. 5b). The rate of air cooling of 10 mm cast iron tiles measured within the 850÷500°C range is identical in both cases and equals 1.23 K/s. The observed effect of austenitisation temperature on the quantitative composition of the structure is confirmed by paper [20].

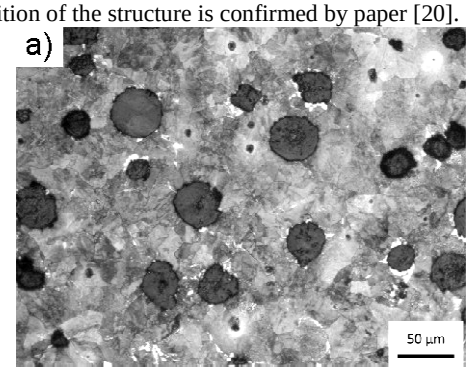

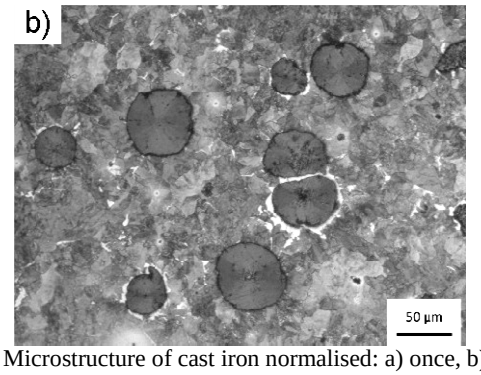

Fig. 5. Microstructure of cast iron normalised: a) once, b) twice

Cast iron normalised in accordance with variant N1 has hardness of 322 HB, for variant N2 - 305 HB. Microhardness of moulded cast iron pearlite is 322 HV0.1, normalised per the N1 variant - 380 HV 0.1, and normalised per the N2 variant - 360 HV0.1.

The fact that cast iron pearlite hardness after single normalisation (380 HV0.1) is greater than after double normalisation (360 HV0.1) can not be explained by inter-plate distance λ, since it is identical in both cases and equals 0.15 µm.

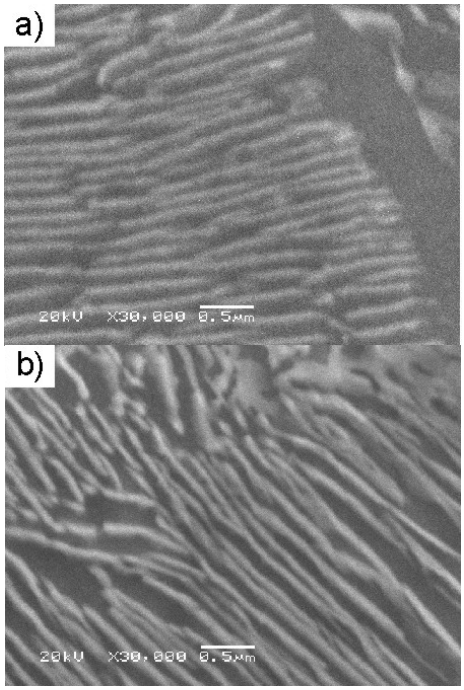

Fig. 6. Pearlite microstructure of cast iron normalised: a) once, b) twice, SEM, micr. zoom 30.000x

It is to be assumed that in both cases (N1 and N2) we are dealing with quasi-pearlite with a ratio of ferrite to cementite quantity ration deviating from the equilibrium (Fig. 6). The ration can be reduced in cast iron cooled from a higher temperature (950°C) due to the greater saturation of austenite with carbon.

The repeated normalisation operation (N2) after austenitisation from a lower temperature aims to break up the

matrix grains, which can grow during austenitisation at 950°C (N1) [21].

Ferrite grain size measurements on samples oversaturated using the random secant method [22] demonstrated that grain size in cast iron normalised once (N1) and twice (N2) is similar and equals 10.5 or 11.3 µm, respectively. Ferrite grains in raw cast iron (S) are highly varied in terms of size, and the average size is 14.9 µm. Ferrite grain size measurement results did not demonstrate growth after austenitisation at 950°C, nor fragmentation due to repeated normalisation with austenitisation at 900°C.

Oversaturation and ageing conditions are the same in all variants of precipitation hardening (Figs. 2-4). During the oversaturation (heating at sub-critical temperature of 720°C for 4 hours), graphitisation and spheroidisation of cementite occurs to a large degree. Graphitisation occurs intensively in moulded cast iron (S, Fig. 7a) or double normalised (N2, Fig. 7e). Ferrite content in cast iron oversaturated per variant S increases to 90.6% v/v, while for variant N2 to 84.8% v/v. The highest pearlite content (ca. 36%) is observed in the matrix of single normalised cast iron (N1). The ferrite-pearlite border is blurred (Fig. 7c). Precise quantitative assessment of ferrite is difficult in this case.

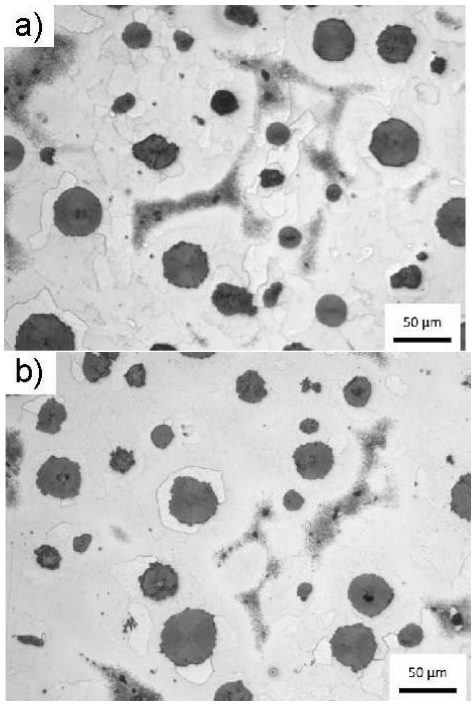

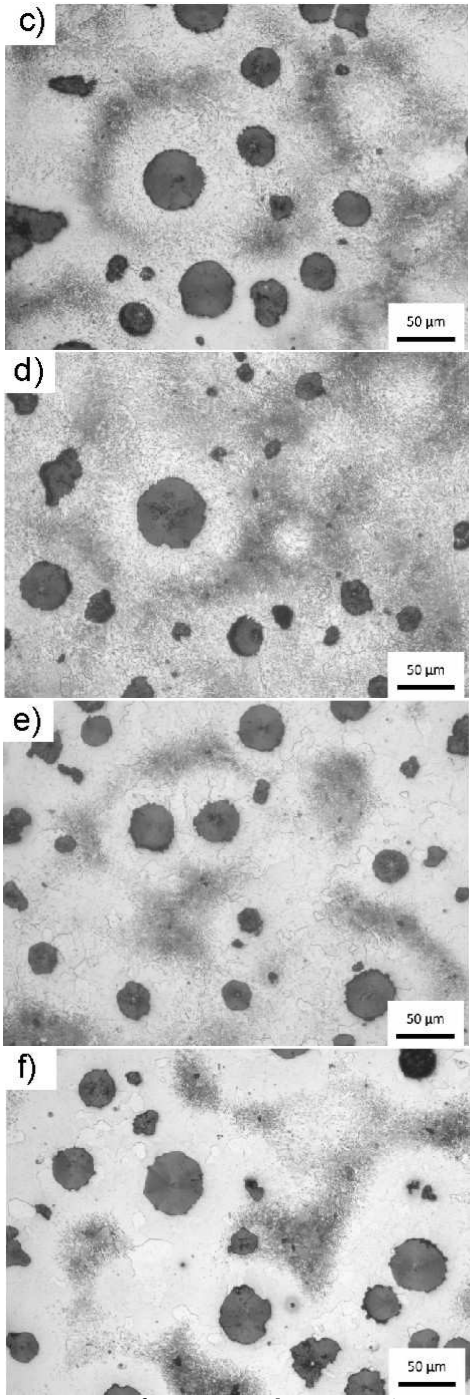

Fig. 7. Microstructure of oversaturated cast iron: a) variant S, c) variant N1, e) variant N2; microstructure of cast iron aged for 32 h: b) variant S, d) variant N1, f) variant N2

The decrease in pearlite content and spheroidisation of eutectoid cementite causes a significant drop in oversaturated cast iron hardness relative to the input state. Hardness of cast iron oversaturated in accordance with variant S is 209 HB (decrease of

40 HB), per variant N1 - 220 HB (decrease of 102 HB), and per variant N2 - 212 HB (decrease of 93 HB).

Cast iron ageing at 450°C does not cause qualitative or quantitative changes in cast iron microstructure observed with a visible spectrum (Fig. 7) or scanning microscope.

Changes of cast iron hardness during ageing are therefore to be solely attributed to precipitation of copper-oversaturated ferrite from ε phase.

Cast iron hardness in relation to ageing time for individual precipitation hardening variants is presented in Fig. 8.

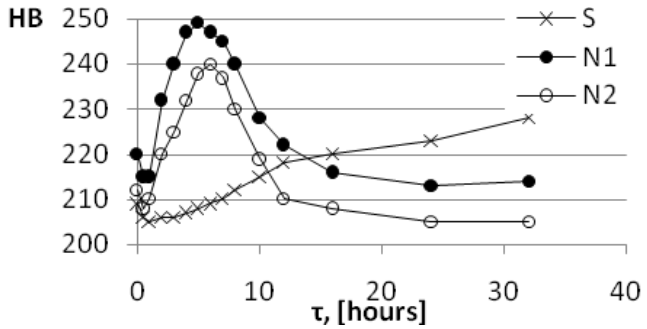

Fig. 8. Cast iron hardness in relation to ageing time

Results of X-ray diffraction tests of selected cast iron samples are presented in Table 4.

Table 4.
Roentgenography test results

Variant	a[1)] / b[2)]	input state	oversaturated state	1 h ageing	32 h ageing
S	a	0.28664	0.28686	0.2868	0.28664
	b	4.844	5.036	4.975	5.15
N1	a	0.28671	0.2869	0.28677	0.28679
	b	5.367	5.385	4.844	4.975
N2	a	0.28664	0.28688	0.2867	0.28666
	b	5.062	5.062	4.844	4.887

[1)] ferrite lattice parameter a, nm,

[2)] half-width $b_{1/2}$ of diffraction line (211), $rd \cdot 10^{-3}$

For the zero value of ageing time, cast iron hardness values were applied for the moment immediately after oversaturation (Fig. 8). During the initial time of ageing (0.5 – 1 h), a slight decrease in hardness is observed in every case. The diffraction line half-width (211) of ferrite decreases (Tab. 4), while the maximum intensity increases. The observed changes in diffraction line parameters can be attributed to a decrease in type 2 stresses and a decrease in point defect density [23]. This is probably the cause of the drop in hardness. The decrease in HSLA steel hardness during the initial period of hardening has been observed by authors of papers [5,6].

Extending the ageing time causes a monotonic increase in hardness of cast iron hardened in accordance with variant S, which reaches 228 HB after 32 hours (Fig. 8). This means a 9.1% increase in hardness, relative to the oversaturated state. In the case of pre-normalised cast iron, hardness reaches its maximum (peak age) after 5 or 6 hours of ageing for variant N1 and N2, respectively. Further extending the ageing time causes a constant decrease in hardness (Fig. 8).

The maximum relative increase in hardness of cast iron hardened per variant N1 or N2 is identical and equals 13.2%. Ageing kinetics assessed by hardness measurements is identical as well. Hardness of cast iron hardened for long periods (24, 32 hours) stabilises at ca. 5÷6 HB belof the hardness of oversaturated cast iron.

The lower hardness of cast iron treated per variant N2 relative to N1 treatment is a result of the lower pearlite content after the oversaturation operation. The highest value of ferrite lattice parameter and the half-width of diffraction line from the (211) planes corresponds to the oversaturated state. In accordance with information from paper [2], copper dissolved in ferrite causes lattice expansion. Short-time ageing (1 h) causes a significant decrease in the lattice parameter, especially in the case of N1 or N2-treated cast iron (Tab. 4). During ageing, the lattice parameter usually reports a decrease. The observed changes are caused by precipitation of ε phase from the oversaturated solution. ε phase particles after ageing for 5 or 6 hours (N1, N2) reach dispersion and dimensions that result in the highest strengthening. Extension of ageing time causes overageing, which results in a constant decrease in hardness. Judging by the plot of hardness relative to the ageing time of cast iron treated per variant S, maximum hardening has not been reached yet after 32 hours.

In light of the acquired results, pre-normalisation of cast iron before oversaturation is fully justified. Austenitisation during normalisation facilitates homogenisation of chemical composition in the cast iron matrix. This results in a fuller oversaturation (Tab. 4) and shorter time until maximum hardness is attained. The sensibility of repeated normalisation is debatable.

4. Conclusions

1. Low-alloy copper-nickel spheroidal cast iron can be successfully precipitation hardened (hardness increase of 9.1-13.2%) using four-hour oversaturation at sub-critical (720°C) temperature with following ageing at 450°C.
2. Pre-normalisation of cast iron shortens the ageing time required to attain maximum hardness to 5 hours. Cast iron reaches maximum hardness (249 HB) and, as has to be assumed, tensile strength that correspond to moulded cast iron. Due to the predominant ferrite content in the matrix, plastic qualities of precipitation hardened cast iron can be superior to moulded cast iron. The above assumptions have to be verified by comprehensive tests of mechanical properties.
3. Precipitation hardening of moulded cast iron is not effective, since the maximum increase in hardness is the lowest (9.1%) and is reached only after 32 hours of ageing.
4. The only significant effect of double pre-normalisation is a more complete ferritisation of the matrix in the course heating during oversaturation. This effect can be achieved by extending the oversaturation time and skipping repeated normalisation.

References

[1] Massalski, T.B. (1990). *Binary Alloy Phase Diagrams*. (2nd ed.). Ohio: ASM International.

[2] Lee, B.J., Wirth, B.D., Shim, J.H., Kwon, J., Kwon, S.C. & Hong, J.H. (2005). Modified embedded-atom method interatomic potential for the Fe-Cu alloy system and cascade simulations on pure Fe and Fe-Cu alloys. *Physical Review B.* 71(18), 184205:1-184205:15. DOI: 10.1103/Phys RevB.71.184205.

[3] Velthuisa, S.G.E., Rootc, J.H., Sietsmab, J., Rekveldta, M. Th. & Van Der Zwaagb, S. (1998). The ferrite and austenite lattice parameters of Fe–Co and Fe–Cu binary alloys as a function of temperature. *Acta mater*. 46(15), 5223-5228. DOI: 10.1016/S1359-6454(98)00248-1.

[4] Martin, J.W., Doherty, R.D. & Cantor, B. (1997). *Stability of microstructure in metallic systems*. (2nd ed.). Cambridge: Cambridge University Press.

[5] Yina, G., Yang, C. & Lud, Y. (2010). HREM Observation of Age-Precipitated Particles in Practical Cu-bearing Ultra-Low Carbon Steels. *Journal of Materials Science & Technology*. 26(5), 433–438. DOI: 10.1016/S1005-0302(10)60068-0.

[6] Bhagat, A.N., Pabi, S.K., Ranganathan, S. & Mohanty, O.N. (2004). Aging Behaviour in Copper Bearing High Strength Low Alloy Steels. *Isij International*. 44(1), 115-122. DOI: 10.2355/isijinternational.44.115.

[7] Dhua, S.K., Ray, A. & Sarma, D.S. (2001). Effect of tempering temperatures on the mechanical properties and microstructures of HSLA-100 type copper-bearing steels. *Materials Science and Engineering: A.* 318(1-2), 197-210. DOI: 10.1016/S0921-5093(01)01259-X.

[8] Ray, P.K., Ganguly, R.I. & Panda, A.K. (2003). Optimization of mechanical properties of an HSLA-100 steel through control of heat treatment variables. *Materials Science and Engineering: A.* 346(1), 122-131. DOI:10.1016/S0921-5093(02)00526-9.

[9] Pytel, S.M. & Rynkar, B. (1997). Low carbon copper-bearing structural steels. In Ist National Scientific Conference (Materials Science -Quality-Foundry), 20-22 February 1997 (pp. 177-184). Cracow, Poland: Institute of Metallurgy and Materials Science. (in Polish).

[10] Lis, J. & Wieczorek, P. (2001). Precipitation strengthening and mechanical properties of ultra low carbon bainitic steel with Cu addition. *Materials Engineering.* 121(2), 96-102.

[11] Kosowski, A., Podrzucki, Cz. (1981). *Alloyed cast iron*. Cracow: Ed. AGH.

[12] Pan, E.N. (1988). Einfluβ von Kupfer, Zinn und mangan aufdie eutektoide Umwandlung von graphitischen Guβeisen. *Giesserei-Praxis.* 15-16, 193-207.

[13] Podrzucki, Cz. (1991). *Cast Iron. Structure, Properties, Application. Vol. 1 and 2*. Cracow: Publishing house ZG STOP.

[14] Richards, L. & Nicola, W. (2003*). Final; technical report: Age strengthening of gray cast iron, phase III. University of Missouri. Report No.DOE/ID13851*. Retrieved May 02, 2014, from http://www.osti.gov/scitech/biblio/812004. DOI: 10.2172/812004.

[15] Szykowny, T., Dymski, S. (2008). Influence of copper on effects of precipitation hardening of ductile cast iron. *Archives of Foundry Engineering.* 8(3), 191-198.

[16] Szykowny, T., Dymski, S., Giętka, T. (2011). The influence of the copper content and precipitation hardening on mechanical properties of nodular cast iron. In S. Pietrowski (Eds.), *High quality Foundry Technologies, Materials and Castings*, (pp.133-142). Katowice-Gliwice: Polish Academy of Science, The Katowice Branch, Commission of Foundry Engineering Gliwice.

[17] Szykowny, T. (1995). Analysis of dispersive hardening of the low Cu–content spheroidal cast iron. *Scientific Papers ATR Mechanics.* 193(38), 131-137.

[18] Szykowny, T. (2003). Investigations of low-copper spheroidal graphite cast iron precipitation hardening. In International Scientific Conference Ductile Iron of the 21ST Century, 2-3 October 2003 (pp. 33-42). Cracow, Poland: Foundry Research Insitute.

[19] Szykowny, T. (1997). Effect of Cu-content and starting microstructure of spheroidal cast iron on the results of dispersive hardening. In VIII International Scientific and Technical Conference, Trends and Development in Manufacturing Processes, September 1997 (pp. 23-28). Zielona Góra, Poland: Publ. PZ.

[20] Szykowny, T. (2003). Ductile Cast Iron Structure Forming During Continuous Cooling. *Archives of Foundry*. 3(8), 111-118.

[21] Jonuleit, A., (1977). Austenitkorngrossendiagram und einige Aspekte des Austenitkornwachstums fűr unlegiertes Gusseisen mit Kugelgraphit. *Gissereitechnik*. 6, 163-170.

[22] Ryś, J. (1995). *Stereology of materials.* Cracow: Fotobit Design.

[23] Rusakov, A.A. (1977). *Roentgenography of Metals.* Moscow: Atomizdat.